Mechanistic Studies of Peroxynitrite-Mediated Tyrosine Nitration in Membranes Using the Hydrophobic Probe *N-t*-BOC-L-tyrosine *tert*-Butyl Ester†

Silvina Bartesaghi,‡ Valeria Valez,‡ Madia Trujillo,‡ Gonzalo Peluffo,‡ Natalia Romero,‡ Hao Zhang,§ Balaraman Kalyanaraman,§ and Rafael Radi*,‡

Departamento de Bioquímica and Center for Free Radical and Biomedical Research, Facultad de Medicina, Universidad de la República, Montevideo 11800, Uruguay, and Biophysics Research Institute and Free Radical Research Center, Medical College of Wisconsin, Milwaukee, Wisconsin 53226

Received February 21, 2006; Revised Manuscript Received March 28, 2006

ABSTRACT: Most of the mechanistic studies of tyrosine nitration have been performed in aqueous solution. However, many protein tyrosine residues shown to be nitrated in vitro and in vivo are associated to nonpolar compartments. In this work, we have used the stable hydrophobic tyrosine analogue *N-t*-BOC-L-tyrosine *tert*-butyl ester (BTBE) incorporated into phosphatidylcholine (PC) liposomes to study physicochemical and biochemical factors that control peroxynitrite-dependent tyrosine nitration in phospholipid bilayers. Peroxynitrite leads to maximum 3-nitro-BTBE yields (3%) at pH 7.4. In addition, small amounts of 3,3′-di-BTBE were formed at pH 7.4 (0.02%) which increased over alkaline pH; at pH 6, a hydroxylated derivative of BTBE was identified by HPLC-MS analysis. BTBE nitration yields were similar in dilauroyl- and dimyristoyl-PC and were also significant in the polyunsaturated fatty acid-containing egg PC. $^{\bullet}OH$ and $^{\bullet}NO_2$ scavengers inhibited BTBE nitration. In contrast to tyrosine in the aqueous phase, the presence of CO_2 decreased BTBE nitration, indicating that $CO_3^{\bullet-}$ cannot permeate to the compartment where BTBE is located. On the other hand, micromolar concentrations of hemin and Mn-tccp strongly enhanced BTBE nitration. Electron spin resonance (ESR) detection of the BTBE phenoxyl radical and kinetic modeling of the pH profiles of BTBE nitration and dimerization were in full agreement with a free radical mechanism of oxidation initiated by ONOOH homolysis in the immediacy of or even inside the bilayer and with a diffusion coefficient of BTBE phenoxyl radical 100 times less than for the aqueous phase tyrosyl radical. BTBE was successfully applied as a hydrophobic probe to study nitration mechanisms and will serve to study factors controlling protein and lipid nitration in biomembranes and lipoproteins.

Peroxynitrite[1] is a powerful oxidant formed in vivo by the diffusion-controlled reaction between nitric oxide ($^{\bullet}NO$) and superoxide radicals ($O_2^{\bullet-}$), and it serves as a pathogenic mediator in a variety of disease states (*1*−*4*). Peroxynitrite can undergo a proton-catalyzed homolysis (*5*, *6*) to nitrogen dioxide ($^{\bullet}NO_2$) and hydroxyl ($^{\bullet}OH$) radicals in ∼30% yields, with a first-order rate constant of $\sim 1\ s^{-1}$ at pH 7.4 and 37 °C (*5*, *7*, *8*). However, in biological systems, the reactivity of peroxynitrite is dictated mainly by direct reactions with different biological targets including thiols (*6*), transition metal-containing centers, and carbon dioxide (CO_2). Importantly, peroxynitrite-mediated one-electron oxidation of heme iron-containing centers ($k = 10^4-10^7\ M^{-1}\ s^{-1}$ at pH 7.4 and 37 °C) leads to the formation of potent secondary oxidants such as oxo−iron ($O{=}Fe^{4+}$) complexes and $^{\bullet}NO_2$, while the reaction with CO_2 ($k = 4.6 \times 10^4\ M^{-1}\ s^{-1}$ at pH 7.4 and 37 °C) yields the transient nitrosoperoxocarboxylate adduct ($ONOOCO_2^-$) (*4*, *9*) which is homolyzed to the carbonate radical ($CO_3^{\bullet-}$) and $^{\bullet}NO_2$ in 33% yields (*8*, *10*, *11*). Thus, $O{=}Fe^{4+}$, $CO_3^{\bullet-}$, and $^{\bullet}NO_2$ ($E°_{O=Fe^{4+}/Fe^{3+}} = 1.4-1.8$ V, $E°_{CO_3^{\bullet-}/CO_3^{2-}} = 1.78$ V, and $E°_{^{\bullet}NO_2/NO_2^-} = 0.99$ V), respectively, can be proximal reactive species in several peroxynitrite-mediated oxidations (*12*−*14*), including protein tyrosine nitration to 3-nitrotyrosine (*1*, *15*).

Protein tyrosine nitration in vivo not only serves as a footprint to unravel the formation and reactions of $^{\bullet}NO$-derived oxidants but in some cases contributes to alterations (loss or gain) of protein function, affects tyrosine kinase-dependent signal transduction cascades, and triggers immunological responses (*1*, *16*). There is an ongoing interest in the identification of nitrated proteins in disease states, in the mapping of nitrated tyrosine residues within a protein, and in defining the biologically relevant mechanisms of nitration (*1*, *17*−*19*). It is now generally agreed that tyrosine nitration occurs by more than one mechanism (e.g., peroxynitrite or hemoperoxidase dependent) but which involves, in all cases, the action of reactive intermediates and/or radical

† This work was supported by grants from the Howard Hughes Medical Institute to R.R. and the National Institutes of Health to B.K. and R.R. (2 R01Hl063119−05). A donation for research support from Laboratorios Gramón-Bagó through Universidad de la República is gratefully acknowledged. S.B. was partially supported by a fellowship from the Ph.D. Program of Facultad de Química, Universidad de la República, Uruguay.

* To whom correspondence should be addressed. Telephone: 598-2-9249561. Fax: 598-2-9249563. E-mail: rradi@fmed.edu.uy.

‡ Universidad de la República.

§ Medical College of Wisconsin.

[1] IUPAC recommended names for peroxynitrite anion ($ONOO^-$) and peroxynitrous acid (ONOOH) ($pK_a = 6.8$) are oxoperoxonitrate(1−) and hydrogen oxoperoxonitrate, respectively. The term peroxynitrite is used to refer to the sum of $ONOO^-$ and ONOOH.

10.1021/bi060363x CCC: $33.50
Published on Web 05/13/2006

species (*1*). In the case of peroxynitrite, $CO_3^{\bullet-}$ and oxo−metal complexes (*1*, *17*, *20*) initially attack the tyrosine phenol moiety to form the tyrosyl (phenoxyl) radical which can react with either $^{\bullet}NO_2$ to form 3-nitrotyrosine or another phenoxyl radical to form 3,3′-dityrosine. Another tyrosine product arising during peroxynitrite-dependent reactions is 3,4-dihydroxyphenylalanine (DOPA),[2] formed by reaction with $^{\bullet}OH$ which preferentially adds to the tyrosine ring instead of performing one-electron abstraction or by reaction with oxo−metal complexes. The yields of 3-nitrotyrosine, 3,3′-dityrosine, and 3,4-dihydroxyphenylalanine vary rather differently as a function of pH, with the largest tyrosine-derived product being 3-nitrotyrosine at physiological pH. Indeed, 3-nitrotyrosine yields are bell-shaped with a maximum around pH 7.4 (*21*); on the other hand, 3,3′-dityrosine yields are minimal at low pH and increase significantly under alkaline conditions (*15*), and 3,4-dihydroxyphenylalanine yields are high at acidic pH and decrease with the pH increase (*22*). So far, and although the pH dependency for peroxynitrite-dependent reactions has been rationalized for a series of biotargets (*6*, *8*, *11*), no kinetic mechanism has been offered to explain these pH dependencies of the yields obtained for the three different tyrosine-derived products. In phosphate buffer, pH 7.4, yields with respect to peroxynitrite are about 6−8% for nitration, 0.24% for dimerization, and 0% for hydroxylation; nitration yields could increase up to 14−16% in the presence of CO_2 and to even higher values in the presence of transition metal complexes (*21*, *23*, *24*).

Most of the mechanistic studies of tyrosine nitration have been performed in aqueous solution. However, many tyrosine residues shown to be nitrated in vitro and in vivo are associated to nonpolar compartments such as biomembranes [e.g., erythrocyte membrane band 3 (*25*), red cell membrane proteins (*26*), complex I of the mitochondrial inner membrane (*27*), sarcoplasmic reticulum Ca^{2+}-ATPase (*28*), and microsomal glutathione *S*-transferase (*29*)] and within the structure of lipoproteins [e.g., Apo A and Apo B (*30*)]. In many of these cases (*27*−*29*) nitration occurs in tyrosines located in transmembrane domains, while in other cases nitration is directed to solvent-exposed tyrosines (*25*) or is decreased after tyrosine association to hydrophobic domains (*30*). Therefore, there is a need to develop and validate hydrophobic probes to study and rationalize nitration processes in hydrophobic environments. In this regard, *N*-*t*-BOC-L-tyrosine *tert*-butyl ester (BTBE) is a stable tyrosine analogue that has been efficiently incorporated (>98%) into the lipid phase of phosphatidylcholine (PC) liposomes with the highest concentration near the glycerol backbone (*31*). Peroxynitrite addition to both multi- and unilamellar liposomes caused formation of both 3-nitro-BTBE and 3,3′-di-BTBE, with the yield of the nitro derivative much higher than that of the corresponding dimer.

Peroxynitrite can diffuse through and interact with biomembranes (*32*, *33*) and lipoproteins (*34*, *35*) and promote oxidation and nitration reactions in protein and lipid targets (*1*, *25*, *36*, *37*). However, mechanistic insights on peroxynitrite-mediated tyrosine nitration in hydrophobic compartments are lacking; some of the assumptions valid for the aqueous phase may not be valid due to the different polarity of the environment and to spatial restrictions and diffusional constraints of both reactants and target molecules, among several other factors. Moreover, the relevance of tyrosine dimerization and, the previously unexplored, hydroxylation in the lipid phase remains to be specifically assessed.[3] Thus, in this work we have used the hydrophobic tyrosine analogue BTBE incorporated into different types of PC liposomes as a probe to study physicochemical and biochemical factors that control peroxynitrite-dependent tyrosine nitration in membrane model systems.

MATERIALS AND METHODS

Chemicals. Diethylenetriaminepentaacetic acid (dtpa), ethylenediaminetetraacetic acid (edta), manganese dioxide, sodium bicarbonate, potassium phosphate, L-tyrosine, desferrioxamine mesylate, α-lipoic acid, *p*-hydroxyphenylacetic acid (pHPA), uric acid, mannitol, hemin, deoxycholic acid, 3-nitrotyrosine, 2-methyl-2-nitrosopropane (MNP), and *N*-acetyltyrosine were purchased from Sigma. *N*-*t*-BOC-L-tyrosine *tert*-butyl ester (BTBE), 3-nitro-*N*-*t*-BOC-L-tyrosine *tert*-butyl ester (3-nitro-BTBE), and 3,3′-di-*N*-*t*-BOC-L-tyrosine *tert*-butyl ester (3,3′-di-BTBE) (see structures in Figure 1) were prepared and handled as previously (*31*). Stock BTBE solutions (1 M) were prepared in methanol immediately before use. 3,3′-Dityrosine was kindly provided by Dr. Stanley Hazen (Cleveland Clinic Foundation). 1,2-Dimyristoyl-*sn*-glycero-3-phosphocholine (DMPC), 1,2-dilauroyl-*sn*-glycero-3-phosphocholine (DLPC), and egg and soybean phosphatidylcholine were from Avanti Polar Lipids. Mn-tccp [manganese(III) *meso*-tetrakis(4-carboxylatophenyl)porphyrin] and Fe-tcpp [iron(III) *meso*-tetrakis(4-carboxylatophenyl)porphyrin] were from Calbiochem. Hydrogen peroxide (H_2O_2) was from Fluka. Organic solvents for synthesis of standards and chromatography were from Baker. All other compounds were of reagent grade.

Stock hemin solution was freshly prepared in 0.1 N NaOH and kept in the dark at 4 °C until use. The ferric iron−edta and ferric iron−desferrioxamine (ferrioxamine) complexes were prepared by mixing equal volumes of edta and desferrioxamine with ferric chloride, respectively, in a concentration ratio of 1.1:1. Mn-tccp and Fe-tcpp stock solutions were 1.21 and 1.10 mM, respectively, and were diluted in 0.1 N NaOH. Fenton chemistry was performed by preparing a stock solution of 10 mM $FeSO_4$ in 2.5 mM H_2SO_4 which was then added to BTBE-containing liposomes in the presence of hydrogen peroxide (H_2O_2) to a final Fe^{2+}:H_2O_2 ratio of 1. All solutions were prepared with highly pure deionized nanopure water to minimize trace metal contamination.

[2] Abbreviations: BOC, *tert*-butyl pyrocarbonate; BTBE, *N*-*t*-BOC-L-tyrosine *tert*-butyl ester; DMPC, 1,2-dimyristoyl-*sn*-glycero-3-phosphocholine; DLPC, 1,2-dilauroyl-*sn*-glycero-3-phosphocholine; dtpa, diethylenetriaminepentaacetic acid; edta, ethylenediaminetetraacetic acid; $ONOO^-$, peroxynitrite; Mn-tccp, manganese(III) *meso*-tetrakis-(4-carboxylatophenyl)porphyrin; Fe-tccp, iron(III) *meso*-tetrakis(4-carboxylatophenyl)porphyrin; PC, phosphatidylcholine; HPLC, high-performance liquid chromatography; MNP, 2-methyl-2-nitrosopropane; DF, desferrioxamine; Fe-DF, ferrioxamine; LA, lipoic acid; pHPA, *p*-hydroxyphenylacetic acid; DMSO, dimethyl sulfoxide; UA, uric acid; GSH, glutathione; ESR, electron spin resonance; LIT, linear ion trap; DOPA, 3,4 dihydroxyphenylalanine; RA, reverse addition.

[3] Throughout this paper, we will refer as BTBE oxidation to the sum of nitration, dimerization, and hydroxylation on the BTBE moiety.

Peroxynitrite Synthesis and Addition. Peroxynitrite was synthesized in a quenched-flow reactor from sodium nitrite ($NaNO_2$) and H_2O_2 under acidic conditions as described previously (*36*). The H_2O_2 remaining from the synthesis was eliminated by treating the stock solutions of peroxynitrite with granular manganese dioxide, and the alkaline peroxynitrite stock solution was kept at −20 °C until use. Peroxynitrite concentrations were determined spectrophotometrically at 302 nm (ϵ = 1670 M^{-1} cm^{-1}). The nitrite concentration in the preparations was typically lower than 30% with respect to peroxynitrite. Control of nitrite levels proved to be critical for obtaining reproducible data (see Results). In some control experiments, peroxynitrite was allowed to decompose to nitrate and nitrite in 100 mM phosphate buffer, pH 7.4, before use, i.e., "reverse order addition" of peroxynitrite (RA).

BTBE Incorporation into Phosphatidylcholine Liposomes. BTBE incorporation into liposomes was carried out as in ref *31* with minor modifications. Briefly, a methanolic solution of BTBE (0.35 mM) was added to 35 mM PC lipids dissolved in chloroform. Under these conditions more than 98% BTBE was incorporated (*31*). The mixture was then dried under a stream of nitrogen gas. Multilamellar liposomes were formed by thoroughly mixing the dried lipid with 100 mM potassium phosphate buffer, pH 7.4, plus 0.1 mM dtpa. Liposomes (0.3 mM BTBE) were exposed to peroxynitrite under different conditions throughout the work. BTBE and BTBE-derived products (e.g., 3-nitro-BTBE and 3,3′-di-BTBE) were extracted with chloroform, methanol, and 5 M NaCl as reported previously [1:2:4:0.4, sample:methanol: chloroform:NaCl (v/v) with recovery efficiencies for all compounds >95% (*31*)]. Samples were then dried and stored at −20 °C. Immediately before HPLC separation, samples were resuspended in 100 μL of a mixture containing 85% methanol and 15% KP_i (15 mM), pH 3. Experiments with liposomes were performed at 37 °C for DMPC and at 25 °C for DLPC, egg PC, and soybean PC, in all cases above the transition phase temperatures (i.e., 23, −1, −3, and <0 °C, respectively).

HPLC Analysis. BTBE, 3-nitro-BTBE, and 3,3′-di-BTBE were separated on a Gilson HPLC system equipped with UV−vis and fluorescence detectors by reverse-phase HPLC using a Partisil ODS-3 10 μm column (250 mm length, 4.6 mm i.d.). Mobile phase A consisted in 15 mM phosphate buffer, pH 3, and mobile phase B consisted in methanol. Chromatographic conditions were as follows: flow, 1 mL/min; 75% mobile phase B for 25 min, followed by a linear increase to 100% mobile phase B for 10 min. UV−vis settings were for BTBE (280 nm, ϵ = 1200 M^{-1} cm^{-1}) and for 3-nitro-BTBE (360 nm, ϵ =1500 M^{-1} cm^{-1}). 3,3′-Di-BTBE was detected fluorometrically at λ_{ex} 294 nm and λ_{em} 401 nm. Authentic 3-nitro-BTBE and 3,3′-di-BTBE were used as standards.

For the detection of 3-hydroxy-BTBE (i.e., 3,4-dihydroxy-*N*-*t*-BOC-L-phenylalanine *tert*-butyl ester), the HPLC protocol was slightly modified. Mobil phase A consisted of water, and the gradient was started at 50% methanol to 100% for 35 min. UV−vis detection was at 280 nm while fluorometric detection was performed at λ_{ex} 280 nm and λ_{em} 306 nm.

Artifactual BTBE nitration during the chromatographic separation procedure due to nitrite-dependent nitration at acidic pH was ruled out by appropriate controls using predecomposed peroxynitrite.

Spectrophotometric Analysis. In some experiments using the saturated fatty acid-containing PC (DLPC, DMPC), 3-nitro-BTBE was quantitated by direct UV−vis measurement. Briefly, liposomes were solubilized with 1.2% deoxycholate (*38*) followed by alkalinization to pH 10 with 5 M NaOH, and 3-nitro-BTBE was measured at 424 nm at pH 10 (ϵ = 4000 M^{-1} cm $^{-1}$). Similarly, 3-nitrotyrosine was measured by absorbance measurements at 430 nm at pH 10 (ϵ = 4100 M^{-1} cm $^{-1}$).

Mass Spectrometry Analysis of Hydroxy-BTBE. Hydroxy-BTBE was analyzed using an Applied Biosystems QTRAP, triple quadrupole-linear ion trap (LIT) mass spectrometer equipped with a turbo ion spray ionization source (ESI). The mass spectrometer was operated in positive mode, and the ESI settings were optimized as follows: ion spray voltage 2500 V, temperature 375 °C; declustering potential 50 V, entrance potential 10 V, nebulizer gas 40 psi; heater gas 25 psi. The samples collected from the HPLC were diluted in acidified methanol (0.1% formic acid) and continuously infused (10 μL min^{-1}) at an estimated concentration of 10 nM. We identified the molecular ion at *m*/*z* 353.2. Fragmentation analysis of hydroxy-BTBE was conducted utilizing the LIT in the enhanced product ion mode of the instrument. Fragmentation experiments of the molecular ion at 353.2 were conducted at different collision-assisted dissociation energies identifying fragments from the parent ion.

ESR Measurements. ESR spectra were recorded at room temperature on a Bruker EMX spectrometer operating at 9.8 GHz. Typical spectrometer parameters were as follows: scan range, 100 G; field set, 3510 G; time constant, 0.64 ms; scan time, 20 s; modulation amplitude, 5.0 G; modulation frequency, 100 kHz; receiver gain, 2×10^5; microwave power, 20 mW. Samples were subsequently transferred to a 100 μL capillary tube for ESR measurements.

General Experimental Conditions. Experiments were typically carried out in the presence of BTBE (0.3 mM) in PC liposomes (30 mM) in 100 mM potassium phosphate plus 0.1 mM dtpa, pH 7.4 and 25 °C unless otherwise stated. When the effect of pH on BTBE oxidation yields was studied, potassium phosphate was also used throughout the pH range to avoid confounding reactivities with other buffer system components. The reported final pH after addition of the alkaline peroxynitrite solution was systematically measured and never increased more than 0.2 units.

Estimation of Peroxynitrite Diffusion Distances in the Liposome Suspensions. Estimation of peroxynitrite diffusion distances was made assuming multilamellar liposomes (20 mg/mL) of a mean external diameter of 1000 nm and five-concentric lamellae (*39*). According to previous data (*40*, *41*) a vesicle concentration can be estimated around 0.20 nM corresponding to 3.65×10^{11} vesicles/mL or 190 μL of liposomes/mL of suspension.

On the basis of a previous model developed in our laboratory (*13*) the average diffusion distance (Δx) of aqueous phase-added peroxynitrite before reaching a liposome vesicle can be calculated as

$$\Delta x = r\sqrt{\frac{3}{4}\left(\sqrt[3]{\frac{4n\pi}{3}}\right)^2 - 1} \qquad (1)$$

where n represents the ratio between the total suspension volume and the total liposome volume and r represents the liposome radius. Solution of this equation yields an Δx value of 1.1 μm. The percentage of added peroxynitrite that could effectively reach a vesicle is determined from the equation:

$$\ln\frac{[ONOO^-]_x}{[ONOO^-]_0} = \frac{-\ln 2(\Delta x^2)}{2D_{ONOO^-}t_{1/2}} \quad (2)$$

where $t_{1/2}$ represents the half-life of peroxynitrite in the extracellular medium and D_{ONOO^-} the diffusion coefficient of peroxynitrite, considered to be similar to that of NO_3^-, 1500 $\mu m^2\ s^{-1}$ (*32*, *42*).

Computer-Assisted Simulations. Computer-assisted simulations were performed using the GEPASI program (*43*).

Data Analysis. All experiments reported herein were reproduced a minimum of three times. Results are expressed as mean values with the corresponding standard deviations. Graphics and data analysis were performed using Origin 6.1.

RESULTS

HPLC and Spectroscopic Analysis of BTBE, 3-Nitro-BTBE, and 3,3′-Di-BTBE. To study biochemical and physicochemical factors that control tyrosine nitration in hydrophobic environments, BTBE was incorporated into PC liposomes which then were treated with peroxynitrite. BTBE-derived products were quantitated by UV−vis and/or fluorometric measurements after either (a) reverse phase-HPLC separation of organic extraction material or (b) deoxycholate solubilization. Figure 1A shows a typical HPLC chromatogram obtained from peroxynitrite-treated samples, where BTBE, 3-nitro-BTBE, and 3,3′-di-BTBE eluted at 7, 9, and 19 min, respectively. Alternatively, spectral analysis of 3-nitro-BTBE after liposome solubilization with 1.2% deoxycholate allowed to carry out direct measurements at the peak absorbance of 424 nm at pH 10 (Figure 1B). In DLPC liposomes and pH 7.4 (Figure 1C), peroxynitrite (0−2 mM) caused a dose-dependent increase in BTBE nitration with yields of ∼3% (e.g., 15 μM 3-nitro-BTBE at 500 μM peroxynitrite), with similar results obtained with both methods. Importantly, while the direct spectrophotometric measurement of 3-nitro-BTBE after deoxycholate solubilization turned to be practical and reproducible for saturated fatty acid-containing liposomes (e.g., DMPC and DLPC), it should not be reliably applied to unsaturated fatty acid-containing liposomes (e.g., egg and soybean PC) since peroxynitrite leads to the formation of other absorbing species in the same spectral region such as nitrated and oxidized lipids (*36*, *44*).

Peroxynitrite-Mediated BTBE Hydroxylation in DLPC Liposomes. While in previous work (*31*) the formation on 3-nitro- and 3,3′-di-BTBE was detected upon treatment with peroxynitrite and the myeloperoxidase/nitrite/hydrogen peroxide systems, formation of hydroxylated derivatives of BTBE was not explored. The hydrophobic analogue of 3,4-dihydroxyphenylalanine named herein as 3-hydroxy-BTBE, should be a more polar compound than BTBE, and therefore chromatographic conditions were adjusted to search for compounds eluting at earlier times than BTBE. Initial experiments with peroxynitrite were performed at pH 6.0 as BTBE hydroxylation arising from ONOOH homolysis would

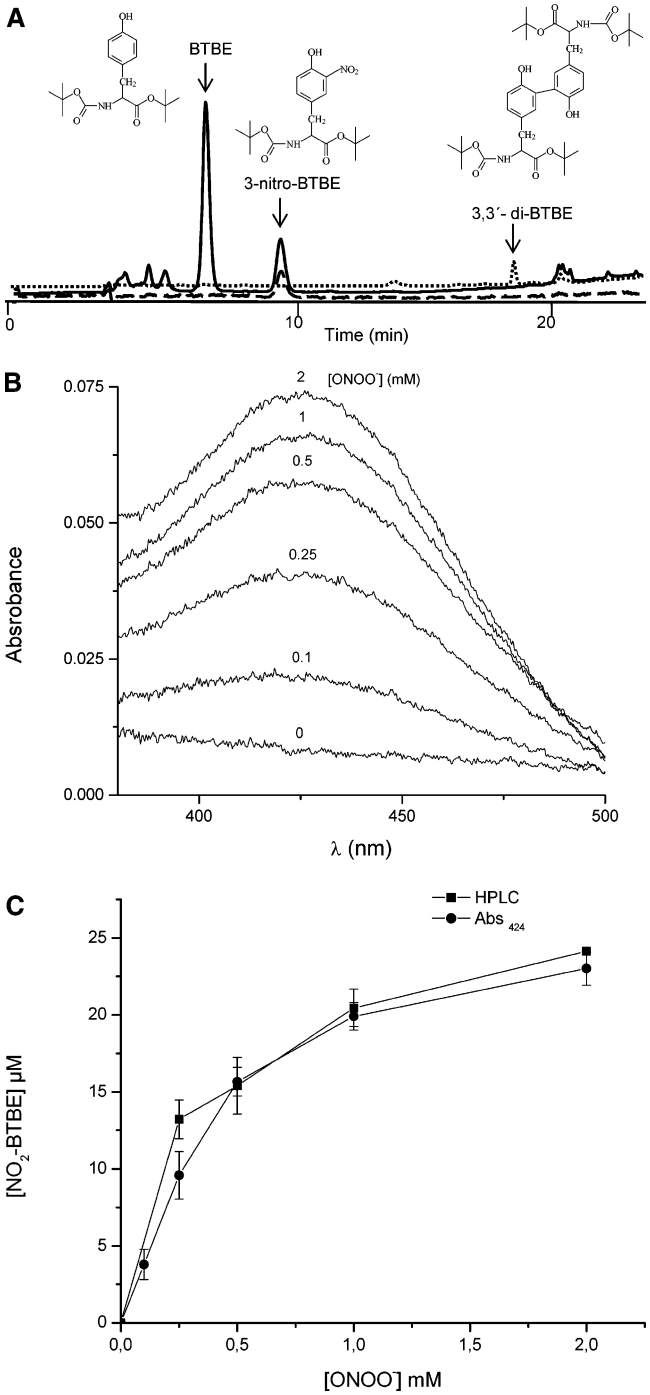

FIGURE 1: Analysis of 3-nitro- and 3,3′-di-BTBE after peroxynitrite addition. BTBE (0.3 mM) in DLPC liposomes (30 mM) was exposed to peroxynitrite in phosphate buffer (100 mM), pH 7.4, plus 0.1 mM dtpa. (A) After an organic extraction, products were separated by RP-HPLC as described under Materials and Methods. The HPLC chromatogram shows the elution of BTBE, 3-nitro-BTBE, and 3,3′-di-BTBE after treatment with $ONOO^-$ (1 mM); the structures have been drawn above the peaks. UV−vis detection was done for BTBE and 3-nitro-BTBE at 280 nm (solid line) and 360 nm (dashed line). 3,3′-Di-BTBE was measured fluorometrically at 294 and 401 nm excitation and emission wavelengths, respectively (dotted line). (B) Peroxynitrite-treated BTBE-containing liposomes were solubilized with 1.2% deoxycholate, the pH was adjusted to 10 with NaOH, and UV−vis spectra of 3-nitro-BTBE were recorded at different peroxynitrite concentrations. (C) Quantitation of 3-nitro-BTBE as a function of peroxynitrite concentration after HPLC separation (■) or deoxycholate solubilization (●).

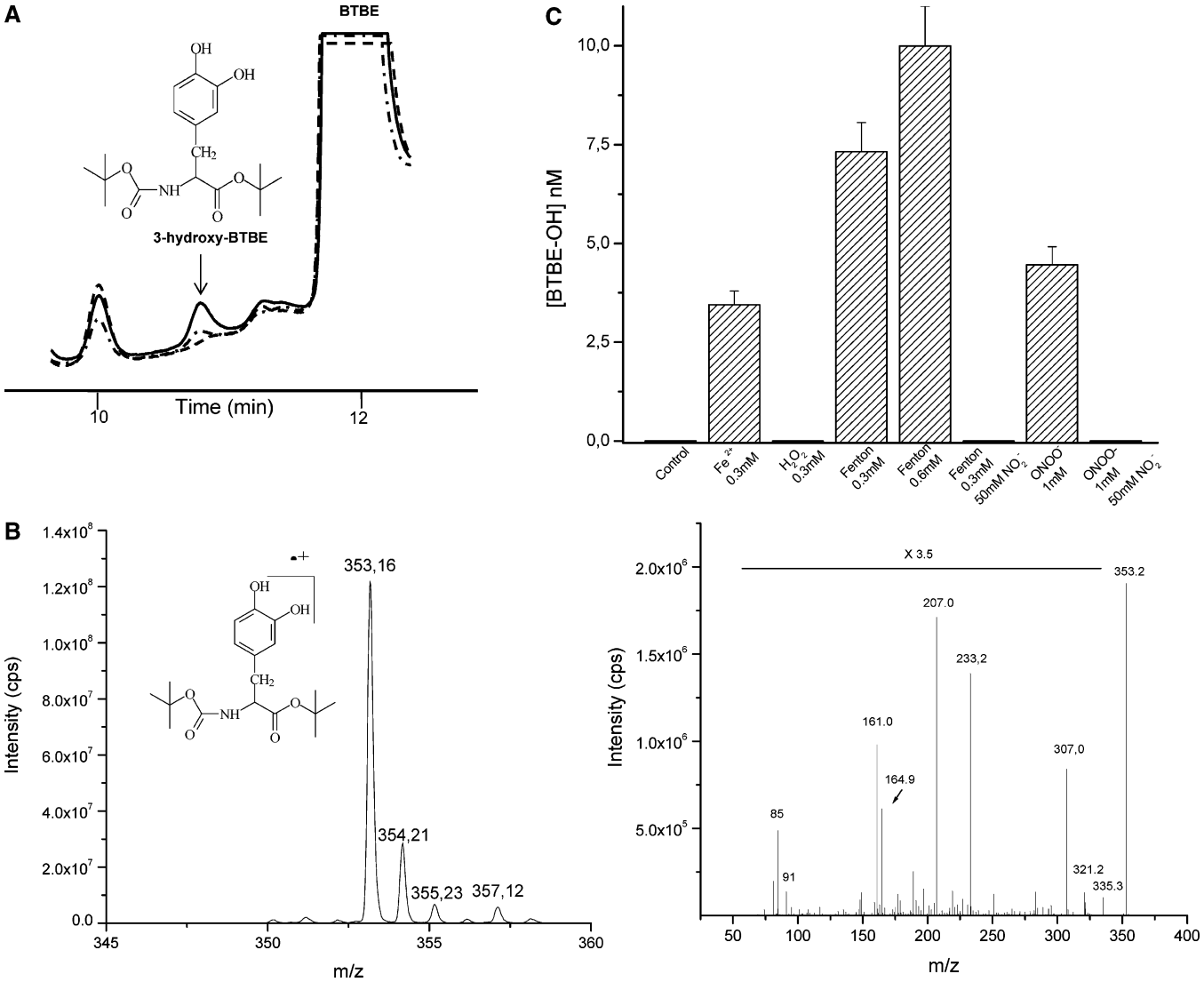

FIGURE 2: HPLC and MS characterization of 3-hydroxy-BTBE. BTBE (0.3 mM) in DLPC liposomes (30 mM) (dashed line) was exposed to $FeSO_4$ (0.3 mM) + H_2O_2 (0.3 mM) (solid line) or peroxynitrite (1 mM) (dot−dashed line) in phosphate buffer (20 mM), pH 6, plus 0.4 mM dtpa. (A) After an organic extraction products were separated by RP-HPLC, and a product eluting immediately before BTBE (12 min) only present in the Fenton and peroxynitrite conditions was obtained as described under Materials and Methods. (B) ES-MS characterization of the peak eluting at 11 min. Left panel: Enhanced resolution mass scan showing the molecular ion at 353.2 and its isotopic distribution. The proposed structure of the compound has been drawn and corresponds to 3-hydroxy-BTBE. Right panel: MS-MS scan (using the LIT) of the ion at *m*/*z* 353.2 showing the fragmentation pattern of 3-hydroxy-BTBE. (C) Quantitation of 3-hydroxy-BTBE formation by a Fenton system or peroxynitrite and the effect of nitrite. The reactions were carried out at pH 6, and conditions are indicated in the graph. 3-Hydroxy-BTBE values were estimated assuming a similar fluorescense quantum yield to that of 3,4-dihydroxyphenylalanine.

be favored under acidic conditions, and additionally, as a positive control of hydroxylation, we used a Fenton system. In both the Fenton and peroxynitrite addition experiments a new peak eluting at 11 min was detected (Figure 2A), which was collected and characterized by MS spectrometry (Figure 2B). Indeed, the molecular mass detected for the peak was *m*/*z* 353.2. Although ES-MS in the positive mode usually produces protonated ions (M + H^+) which would yield a principal ion for hydroxy-BTBE of *m*/*z* 354.2, we detected the molecular ion as happens with *N*-acetyltyrosine (data not shown) and α-tocopherol (*45*, *46*). The absence of a protonatable group and the readily oxidizable phenolic moiety in BTBE favors this type of ionization. The ion *m*/*z* 353.2 corresponds to the molecular radical cation of a hydroxylated derivative of BTBE that we assign as 3-hydroxy-BTBE by analogy with the preferential hydroxylation site of tyrosine and phenolic compounds in general (*22*, *47*). Importantly, the fragmentation pattern of the parent ion at *m*/*z* 353.2 was identical for samples obtained from the Fenton or peroxynitrite addition to liposomes preloaded with BTBE. Among the fragments, one with a *m*/*z* of 335.3 could correspond to the loss of a water molecule from the parent ion. Assuming the fluorescence quantum yield of 3-hydroxy-BTBE to be similar to that of 3,4-dihydroxyphenylalanine, it can be calculated that approximately 5 nM product was formed from 1 mM peroxynitrite at pH 6.0, indicating a low-yield process. No hydroxylated derivative was measured when reactions were conducted at pH 7.4. Figure 2C shows a comparative quantitation of the hydroxylated BTBE derivative formed under different conditions. Hydroxylation in the presence of ferrous iron is due to its fast oxidation to yield $O_2^{\bullet-}/H_2O_2$ under aerobic conditions, thus secondarily generating a Fenton reagent; however, H_2O_2 alone was unable to hydroxylate BTBE, compatible with the need of an iron-

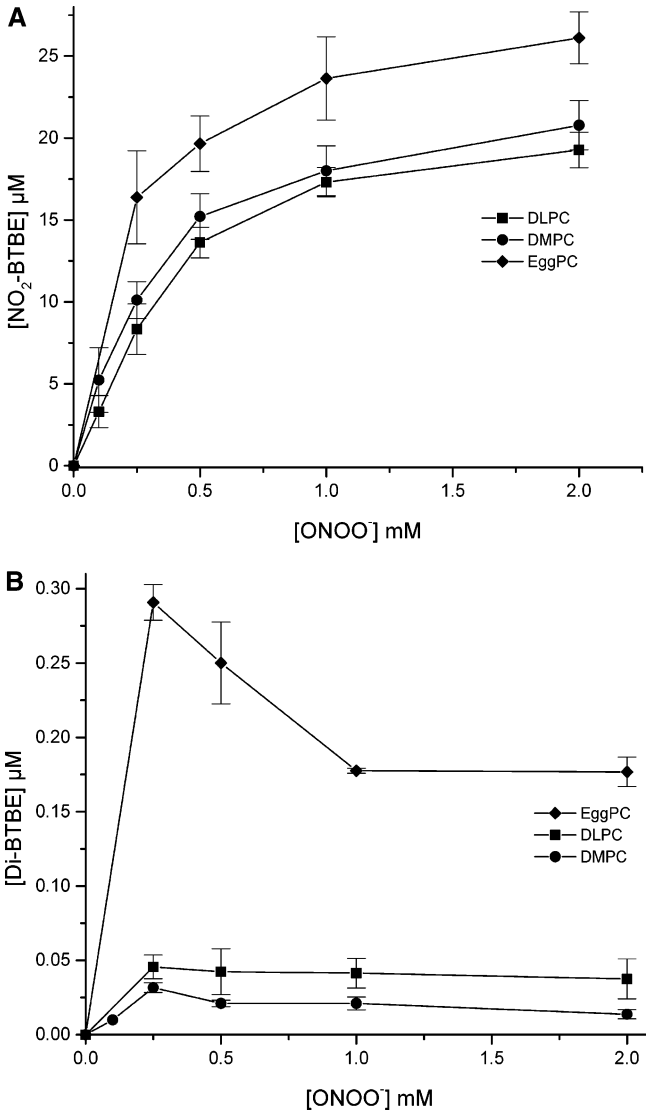

FIGURE 3: Peroxynitrite-mediated BTBE nitration and dimerization in PC liposomes with different degrees of fatty acid unsaturation. BTBE (0.3 mM) in DLPC (■), DMPC (●), and egg PC (◆) liposomes (30 mM) was treated with different concentrations of peroxynitrite in phosphate buffer (100 mM), pH 7.4, plus 0.1 mM dtpa; incubation temperatures were 21 °C for all liposomes except for DMPC, which was incubated at 37 °C. (A) 3-Nitro-BTBE and (B) 3,3′-di-BTBE were measured after RP-HPLC separation. For DLPC and DMPC direct spectrophometric measurements after 1.2% deoxycholate solubilization were also performed, yielding similar results.

catalyzed reaction to yield •OH. While Fenton systems promoted hydroxylation with yields which were dependent on concentration of reagents (i.e., 0.3 and 0.6 mM), the presence of nitrite (NO_2^-) which readily reacts with •OH to yield $^{\bullet}NO_2$ ($k = 6 \times 10^9$ M^{-1} s^{-1}) was fully inhibitory. Peroxynitrite (1 mM) also caused BTBE hydroxylation, with somewhat less efficiency than the Fenton system, and, again, the presence of NO_2^- was completely inhibitory.

While in Figures 1 and 2 the formation of the three BTBE oxidation products by peroxynitrite, i.e., 3-nitro-BTBE, 3,3′-di-BTBE, and 3-hydroxy-BTBE, was established, ESR studies using the spin trap MNP revealed the transient formation of the BTBE phenoxyl radical (Supporting Information, Figure 1S).

Peroxynitrite-Mediated BTBE Oxidation in Saturated and Unsaturated Fatty Acid-Containing Liposomes. Peroxynitrite-derived •OH and $^{\bullet}NO_2$ readily react with unsaturated fatty acids (*36*, *37*); therefore, we investigated the extents of BTBE nitration and dimerization in PC liposomes of different fatty acid composition. Peroxynitrite (0−2 mM) caused a dose-dependent increase in BTBE nitration and oxidation products in DLPC, DMPC, and egg PC liposomes with preincorporated BTBE (Figure 3A). BTBE nitration yields were similar in DLPC and DMPC liposomes while, surprisingly, nitration yields were slightly higher in egg PC liposomes despite the substantial percentage of polyunsaturated fatty acids (∼24%) present in this phospholipid (*39*). On the other hand, BTBE nitration was low (∼4.8 μM 3-nitro-BTBE for 500 μM peroxynitrite) in soybean PC that contains the highest level of polyunsaturated fatty acids (57%) (data not shown). In any event, 3-nitro-BTBE was formed after peroxynitrite addition to all four classes of PC liposomes.

In addition, peroxynitrite caused oxidation of BTBE to yield the corresponding dimer, 3,3′-di-BTBE, being the maximal yields at 250 μM peroxynitrite and higher for egg PC than for DLPC (∼0.11% and 0.02%, respectively; Figure 3B). The dose−response profile of BTBE dimerization was similar to that of tyrosine, which presented higher maximal yields (∼0.24%) at 200 μM peroxynitrite (*31*). In all cases, BTBE nitration yields were significantly higher than those of dimerization at pH 7.4, providing support to the concept that nitration is by far the predominant oxidative modification of tyrosine in membranes challenged with peroxynitrite at physiologically relevant pH (*31*).

Inhibition of Peroxynitrite-Mediated BTBE Oxidation by Scavengers and Carbon Dioxide. To explore the nitration mechanism by peroxynitrite of the membrane-associated hydrophobic tyrosine analogue, we studied the effect of selected scavengers that react with known rate constants with peroxynitrite and/or its derived radicals, namely, •OH and $^{\bullet}NO_2$ (Table 1). While most of the tested scavengers are polar and will mainly react in the aqueous phase, lipoic acid has a hydrophobic character and could undergo reactions in the

Table 1: Effect of Different Scavengers on BTBE Nitration and Dimerization[a]

condition[b]	NO_2-BTBE (μM)	di-BTBE (μM)
$ONOO^-$ (0.5 mM)	9.06 ± 0.78	0.017 ± 0.002
+GSH (0.1 mM)	5.1 ± 1.0	ND
+GSH (1.0 mM)	1.65 ± 0.26	ND
+LA (0.1 mM)	1.32 ± 0.01	0.011 ± 0.002
+pHPA (0.3 mM)	5.60 ± 0.77	0.012 ± 0.002
+tyrosine (1 mM)	4.10 ± 0.66	ND
+DMSO (10 mM)	6.59 ± 0.60	0.006 ± 0.001
+mannitol (50 mM)	2.15 ± 0.87	0
+uric acid (0.3 mM)	0	0
+DTPA (0.1 mM)	9.8 ± 1.1	0.007 ± 0.001
+DF (0.1 mM)	0.71 ± 0.15	0
+nitrite (50 mM)	5.6 ± 1.1	ND
+HCO_3^- (25 mM)	2.32 ± 0	0.008 ± 0
reverse addition of $ONOO^-$	0	0

[a] BTBE (0.3 mM) in DLPC liposomes (30 mM) was exposed to peroxynitrite (0.5 mM) in the presence of the different indicated compounds and concentrations, and 3-nitro-BTBE and 3,3′-di-BTBE were analyzed after RP-HPLC. In the cases where only 3-nitro-BTBE values are provided, direct measurements were made after deoxycholate solubilization. Reverse addition of peroxynitrite represents a control condition with predecomposed peroxynitrite in buffer. ND: not determined. [b] The individual rate constants of the tested scavengers with peroxynitrite, •OH and $^{\bullet}NO_2$, are indicated in Supporting Information (Table 2S).

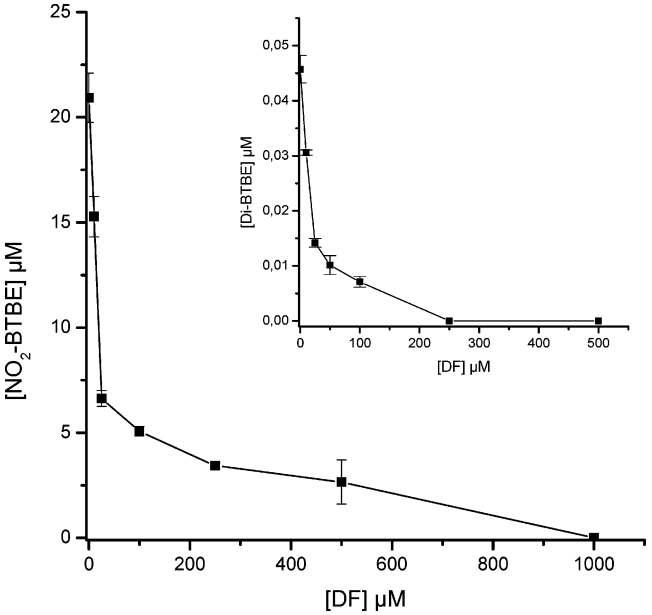

FIGURE 4: Desferrioxamine inhibition of BTBE nitration. BTBE (0.3 mM) in DLPC liposomes (30 mM) was exposed to different concentrations of desferrioxamine (0−1 mM) and treated with peroxynitrite (0.5 mM). 3-Nitro-BTBE was quantitated by UV−vis measurement after RP-HPLC separation of organic extraction products of liposome suspensions. Inset: 3,3′-Di-BTBE was measured fluorometrically after RP-HPLC.

lipid phase or in the aqueous/lipid interphase (*48*). BTBE nitration and dimerization were inhibited by glutathione, lipoic acid, pHPA, tyrosine, DMSO, mannitol, and uric acid in extents that are compatible with their different reactivities with peroxynitrite and peroxynitrite-derived radicals (see Supporting Information, Tables 1S and 2S). The metal chelator dtpa did not affect BTBE nitration (Table 1), but desferrioxamine was capable to potently and dose-dependently inhibit 3-nitro-BTBE and 3,3′-di-BTBE formation (Figure 4) in extents that are consistent with its reactions with $^{\bullet}OH$ and $^{\bullet}NO_2$ (*49*) (Supporting Information, Figure 4S). Notably, the presence of NO_2^- was also inhibitory of nitration, underscoring the role of $^{\bullet}OH$ radicals in the formation of 3-nitro-BTBE, despite a larger formation of $^{\bullet}NO_2$ in this condition.

Table 2: Effect of Transition Metal Complexes on BTBE Nitration[a]

	NO_2-BTBE (μM)	
condition	DLPC	egg PC
$ONOO^-$ (0.5 mM)	14.1 ± 1.9	18.0 ± 2.8
+Fe-EDTA (0.1 mM)	22.5 ± 2.2	7.5 ± 1.7
+Fe-DF (0.1 mM)	15.2 ± 1.1	ND
+hemin (25 μM)	78.0 ± 5.5	97.1 ± 4.4
+Mn-tccp (20 μM)	41.2 ± 1.2	20.6 ± 2.0
+Fe-tccp (50 μM)	31.5 ± 5.0	5.71 ± 0.05
reverse addition of $ONOO^-$	0	0

[a] BTBE (0.3 mM) in DLPC and egg PC liposomes (30 mM) were incubated with the indicated transition metal complexes and concentrations and treated with peroxynitrite (0.5 mM). Samples were analyzed for 3-nitro-BTBE content after RP-HPLC.

Importantly, while bicarbonate/carbon dioxide typically increase tyrosine nitration in aqueous phase (*1*, *11*, *50*) due to a more efficient formation of tyrosyl radical promoted by $CO_3^{\bullet-}$ (*1*), the presence of bicarbonate (25 mM) decreased the nitration of liposome-incorporated BTBE (Table 1). Moreover, bicarbonate inhibited BTBE nitration and dimerization (Figure 5, left and right panels) in a dose-dependent manner.

Transition Metal Complexes Catalyze Peroxynitrite-Dependent BTBE Nitration. Some transition metal complexes enhance peroxynitrite-mediated nitration of phenolic compounds in aqueous environments via a catalytic redox cycle mechanism (*1*, *23*). We studied the effect of different transition metal complexes on peroxynitrite-dependent BTBE nitration and dimerization in saturated (DLPC) and unsaturated (egg PC) liposomes. In DLPC liposomes nitration yields were enhanced in the presence of hemin, Fe-edta, and the metal porphyrins Mn-tccp and Fe-tcpp, while ferrioxamine had no stimulatory effect. In egg PC liposomes, hemin and Mn-tccp enhanced BTBE nitration, while Fe-edta and Fe-tcpp did not (Table 2). It is clear that, in the more simple system containing saturated phospholipids (DLPC), redox-active metal complexes served as nitration catalysts. Indeed, in DPLC liposomes hemin and Mn-tccp enhanced peroxynitrite-dependent BTBE nitration (Figure 6) and dimerization (not shown) in a dose-dependent manner. In particular, hemin

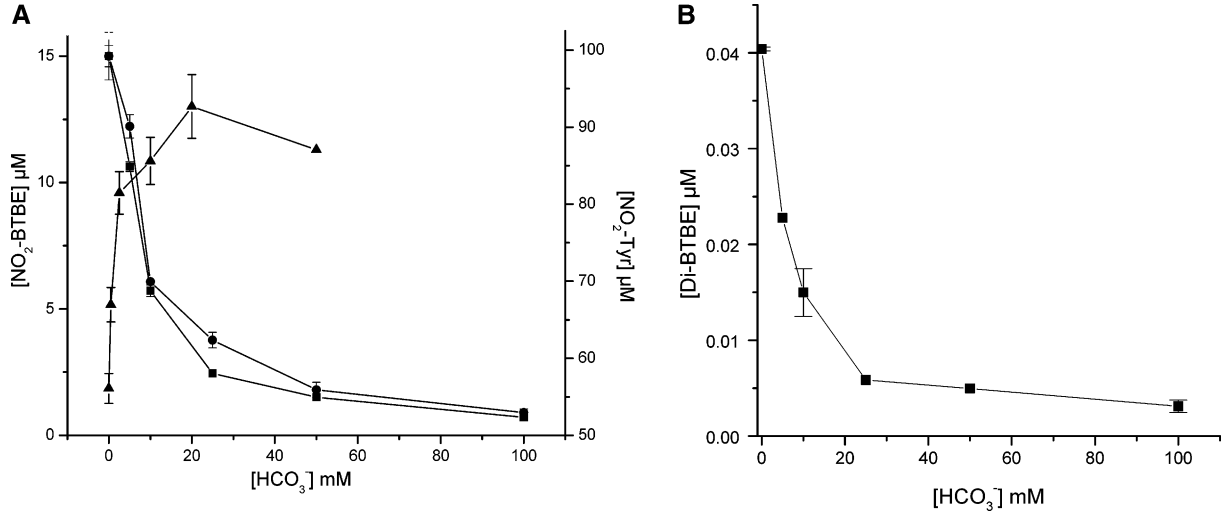

FIGURE 5: Bicarbonate modulation of BTBE and tyrosine nitration. BTBE (0.3 mM) in DLPC liposomes (30 mM) was treated with peroxynitrite (0.5 mM) at different concentrations of bicarbonate (0−100 mM) in phosphate buffer (100 mM). (A) BTBE nitration and (B) dimerization products were analyzed by UV−vis after either RP-HPLC (■) or 1.2% deoxycholate solubilization of liposomes (●). (A) 3-Nitrotyrosine (▲) was measured directly by spectrophotometry.

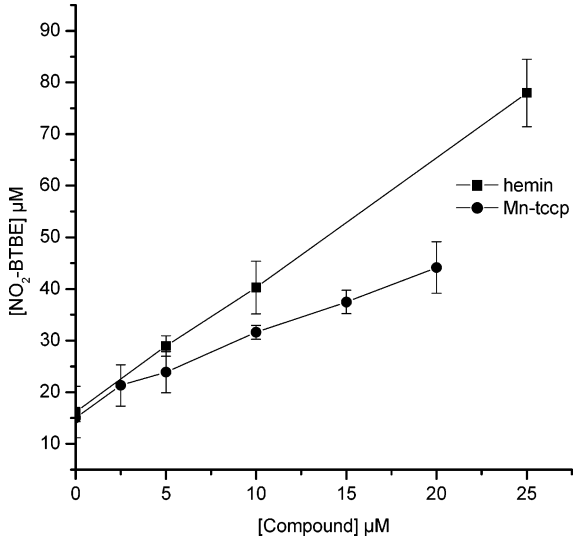

FIGURE 6: Hemin and Mn-tccp catalysis of BTBE nitration. BTBE (0.3 mM) in DLPC liposomes (30 mM) was treated with peroxynitrite (0.5 mM) in the presence of different concentrations of hemin (■) or Mn-tccp (●) at pH 7.4, and samples were analyzed for 3-nitro-BTBE content after RP-HPLC.

was a potent catalyzer, causing an ~5-fold increase in nitration yields (15% at pH 7.4) at 25 μM.

Effect of pH on BTBE Nitration, Dimerization, and Hydroxylation Yields. The effect of pH on BTBE nitration and dimerization was studied to determine to what extent its incorporation into a hydrophobic environment affects the dependency observed for tyrosine. Changes in pH will alter the proton concentration in the aqueous phase and may indirectly influence the chemistry of BTBE occurring in the liposomes. Formation of 3-nitro-BTBE as a function of pH resulted in a bell-shaped curve with a maximum yield at pH 7.5 (Figure 7A) and comparable to that of 3-nitrotyrosine; 3,3′-di-BTBE formation was very low at pH <8 but significantly increased toward alkaline pH (Figure 7B). As indicated previously, 3-hydroxy-BTBE was detected at pH 6 (Figure 2C) but not at pH 7.4. The pH profiles of tyrosine and BTBE nitration, dimerization, and hydroxylation were fully reproduced in silico by computer-assisted simulations considering a free radical mechanism of peroxynitrite-mediated tyrosine oxidations (*1*, *8*, *11*) and a relatively slow dimerization rate constant for the BTBE-phenoxyl radicals (see Supporting Information, Table 1S and Figures 2S and 3S).

On the other hand, the pH profiles of BTBE nitration presented a completely different behavior in the presence of hemin and Mn-tccp, which resulted in a continuous increase of 3-nitro-BTBE toward alkaline pH (Figure 8), reaching nitration yields of 17% and 20%, respectively, at pH 9.

DISCUSSION

In this work we have used the hydrophobic tyrosine analogue BTBE to establish mechanisms of peroxynitrite-mediated tyrosine nitration in membranes and explore factors that control the extents of nitration as well as other oxidative modifications, i.e., tyrosine dimerization and tyrosine hydroxylation. Herein, we confirmed that peroxynitrite was able to induce the formation of 3-nitro-BTBE and 3,3′-di-BTBE in DLPC liposomes (Figure 1) and, importantly, a hydroxylated derivative of BTBE, assigned as 3-hydroxy-BTBE, was

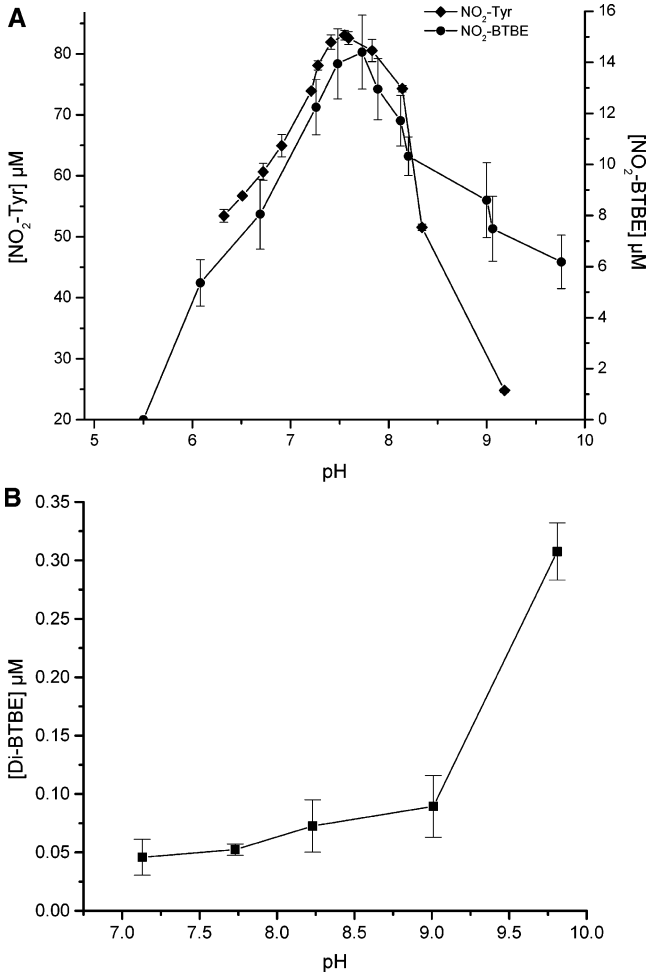

FIGURE 7: BTBE and tyrosine oxidation as a function of pH. DLPC liposomes containing BTBE were prepared after lipid resuspension in phosphate buffer (100 mM) plus 0.1 mM dtpa at different pHs. Then, BTBE (0.3 mM) or tyrosine (0.3 mM) was treated with peroxynitrite (0.5 mM) under different pHs. (A) 3-Nitro-BTBE (●) and (B) 3,3′-di-BTBE (■) were analyzed after organic extraction by RP-HPLC, while in (A) 3-nitrotyrosine (◆) was measured directly by spectrophotometry.

for the first time detected (Figure 2). At pH 7.4, nitration was the predominant process with 3% yield with respect to peroxynitrite in DPLC liposomes (versus 6−8% for free tyrosine) as compared to dimerization (0.02% yield) and hydroxylation (0% yield). In addition to being formed in saturated fatty acid-containing liposomes (DLPC and DMPC), 3-nitro-BTBE was also present in egg (Figure 3) and soybean PC (data not shown), containing substantial amounts of polyunsaturated fatty acids which are readily oxidizable by peroxynitrite-derived species (*36*, *37*). Moreover, despite being modest, dimerization yields were even higher in egg PC than in DLPC liposomes (Figure 3B), which suggests that secondary processes such as lipid peroxidation may participate in BTBE oxidation reactions when polyunsaturated fatty acids are present (see below).

Tyrosine in aqueous solution does not react directly with peroxynitrite (*51*), and thus formation of 3-nitrotyrosine depends on reactions of peroxynitrite-derived radicals ($^{\bullet}OH$, $^{\bullet}NO_2$, $CO_3^{\bullet-}$) (*1*). In the case of BTBE nitration, the data also support a free radical mechanism initiated by the homolysis of ONOOH either in close proximity or inside the membrane. First, BTBE hydroxylation (Figure 2) is

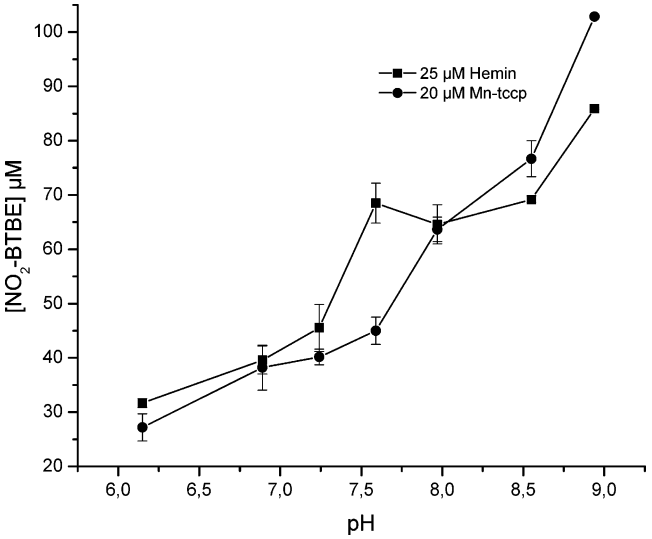

FIGURE 8: Effect of pH on metal complex-catalyzed BTBE nitration. DLPC liposomes containing BTBE were prepared as in Figure 7 and exposed to peroxynitrite (0.5 mM) in the presence of hemin (25 μM) and Mn-tccp (20 μM) at different pHs.

explained by addition of $^{\bullet}$OH to BTBE in the immediacy of the site of homolysis as $^{\bullet}$OH reacts with target molecules within a few molecular diameters of its site of formation; $^{\bullet}$OH, formed from ONOOH in the aqueous phase, is able to penetrate PC vesicles and react with aromatic probe molecules incorporated in the membrane interior as previously shown in water radiolysis studies (*52*); importantly, $^{\bullet}$OH could be also formed inside the liposomes as ONOOH permeates the lipid bilayer (*32*, *33*), and we have previously established the homolysis of ONOOH in aprotic solvents (*31*). Second, inhibitions in nitration and dimerization (Table 1 and Supporting Information) could be explained, in good part, on the basis of simple competition kinetics with free radical scavengers.[4] Third, the detection of the BTBE-derived phenoxyl radical and the pH profile of nitration was fully consistent with a free radical mechanism of reaction leading to the observed BTBE oxidative modifications.

Importantly, to our knowledge this is the first report where the processes of tyrosine (and tyrosine analogue) nitration, dimerization, and hydroxylation from the proton-catalyzed homolysis of peroxynitrite as a function of pH are rationalized with a kinetic model involving free radical reactions[5] (Figure 7 and Supporting Information). Both, the pH profiles and yields of oxidation obtained in silico agree well with the experimental in vitro data for tyrosine and BTBE. In the case of BTBE, the actual rate constants of its reactions with the primary radicals (i.e., $^{\bullet}$OH, $^{\bullet}NO_2$) are not known and were assumed to be the same as for tyrosine; however, for the dimerization reaction (i.e., combination of two BTBE-derived phenoxyl radicals to form 3,3′-di-BTBE), the rate constant value was lowered 100-fold ($k = 2.25 \times 10^6$ M^{-1} s^{-1}) with respect to the corresponding one of tyrosyl radicals ($k = 2.25 \times 10^8$ M^{-1} s^{-1}) due to the restricted lateral motion of molecules in the organized membrane bilayer, which results in a low yield of dimerization with respect to nitration (Figures 3 and 7 and Supporting Information). Indeed, while the diffusion coefficient (D) value of amino acids such as tyrosine in the aqueous phase is in the order of 800−1000 μm^2 s^{-1} (*42*), the estimated D for BTBE in PC liposomes can be safely assumed as ~5 μm^2 s^{-1} as extrapolated from data obtained with the hydrophobic fluorescence aromatic probe pyrene (*53*), inferring a 100−200-fold decrease in tyrosyl radical diffusion in the membrane. Intermolecular tyrosine dimerization will be even less likely in integral peptides and proteins as D values become $>10^3-10^4$ times smaller than in solution (*53*, *54*) and in line with recent data reporting a lack of tyrosine dimerization in peroxynitrite-treated transmembrane peptides (*55*). On the other hand, $^{\bullet}$NO and $^{\bullet}NO_2$ concentrate 4−5-fold in hydrophobic environments, and the apparent D value ($D'_{NO} = 1500$ μm^2 s^{-1}) is very close to that of the aqueous phase of 4500 μm^2 s^{-1} (*56*). The kinetic model proposed herein also predicts that the phenolic hydroxyl group of liposome-incorporated BTBE plays a role, as in the case of tyrosine, in the pH dependency ($pK_a \sim 10$) and that there is no need to invoke other dissociable moieties present in PC such as the phosphate and choline moieties of the polar headgroup. Thus, the kinetic data support that liposomal BTBE accommodates its hydroxyl group toward the lipid/water interphase, in agreement with the structural data (*31*) indicating that the highest concentration of BTBE is present near the glycerol backbone of the phospholipid.

In contrast to what is observed with tyrosine (Figure 5), the presence of bicarbonate decreased BTBE nitration (and dimerization, Figure 5). In heterogeneous systems the presence of bicarbonate may limit the oxidant actions of peroxynitrite (*11*, *13*, *50*) by mechanisms that involve the fast reaction of $ONOO^-$ with CO_2 in the aqueous phase. At 25 mM bicarbonate at pH 7.4 (1.3 mM CO_2) and 25 °C, the half-life of peroxynitrite is reduced from 2.7 s to 24 ms (*13*, *50*), corresponding to an average diffusion distance in homogeneous solution of ~8.5 μm. However, as indicated in Materials and Methods and from eq 1, under the vesicle concentration of our experiments (i.e., 3.65×10^{11} vesicles/mL), the average peroxynitrite diffusion distance to a liposome (Δx) is only 1.1 μm. Thus, according to eq 2 in the presence of 1.3 mM CO_2 less than 2% of added peroxynitrite will react with CO_2 before finding a liposome vesicle. Even at the highest CO_2 concentrations tested (5.4 mM CO_2 in equilibrium with 100 mM HCO_3^-, Figure 5) less than 5% of peroxynitrite diffusion will be inhibited by external CO_2. Thus, added peroxynitrite had access to the vesicles in the suspension under all of the experimental conditions, and the inhibition of BTBE oxidations by CO_2 cannot be a consequence of diffusion limitations due to shortening of peroxynitrite lifetime as previously (*13*, *50*) but is due to a more subtle reason. Peroxynitrous acid, but not peroxynitrite anion, permeates the liposomal membrane (*32*, *33*, *41*); however, ONOOH acid does not react directly with either PC or BTBE, and therefore its consumption inside the membrane will depend only on homolysis to $^{\bullet}$OH and $^{\bullet}NO_2$, which will be rate-limiting and relatively slow; in this scenario, a quasi-equilibrium will be established between

[4] For instance, the data on desferrioxamine (Figure 4 and Supporting Information) provide mechanistic support to a previous report showing inhibition of red cell membrane protein tyrosine nitration by desferrioxamine during exposure to $^{\bullet}NO_2$ gas (26).

[5] In one previous paper (*11*), kinetic modeling of tyrosine nitration as a function of pH was performed in the presence of CO_2. Under this condition ($+CO_2$), the reaction has a pH dependency substantially different from the H^+- or metal-catalyzed nitration reported herein and elsewhere (*15*, *23*) with larger values of nitration at acidic pH.

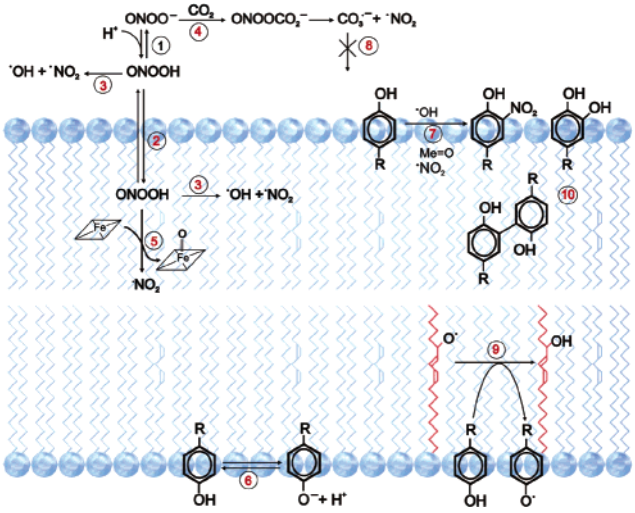

FIGURE 9: Proposed mechanism of nitration of the hydrophobic tyrosine analogue BTBE in phosphatidylcholine bilayers. Peroxynitrite anion ($ONOO^-$) added in the aqueous phase is in equilibrium ($pK_a = 6.8$) with peroxynitrous acid (ONOOH) (1), and ONOOH can readily permeate the phospholipid bilayer (2); ONOOH can undergo homolysis in either the aqueous or lipid phases (3), and $ONOO^-$ can react with CO_2 only in the aqueous phase (4) to yield a transient adduct followed by formation of $CO_3^{\bullet -}$ and $^\bullet NO_2$. In the lipid phase, ONOOH could react directly with hemin to yield the $O{=}Fe^{4+}$ metal complex and $^\bullet NO_2$ (5). BTBE is incorporated into the bilayer, accommodating its phenolic hydroxyl group toward the lipid−water interphase (6) and can undergo a one-electron oxidation to the BTBE phenoxyl radical by either $^\bullet OH$ or the oxo−metal complex (Fe or Mn) followed by reaction with $^\bullet NO_2$ (7). $CO_3^{\bullet -}$ formed in the aqueous phase does not permeate into the hydrophobic compartment where BTBE is located (8). In the presence of polyunsaturated fatty acids, the primary radicals will preferentially initiate lipid peroxidation, and we propose that lipid alkoxyl (9) and peroxyl radicals are responsible of a significant fraction of BTBE one-electron oxidation. In addtition to 3-nitro-BTBE, the formation (in lower yields) of 3,3′-di-BTBE and 3-hydroxy-BTBE is indicated (10).

peroxynitrite in the aqueous and lipid phases (*41*) (Figure 9). In the presence of CO_2, only the fraction of peroxynitrite anion present in the aqueous phase will readily react to yield $ONOOCO_2^-$ and the resulting $CO_3^{\bullet -}$ and $^\bullet NO_2$ radicals. The negatively charged $CO_3^{\bullet -}$ ($pK_a < 0$) (*57*) is incapable of permeating the lipid bilayer (*41*) to promote the one-electron oxidation of BTBE as has been also well established in studies of the reaction of PC membranes with other radical anions such as $Br_2^{\bullet -}$ and $Cl_2^{\bullet -}$ (*52*). As the "extraliposomal" peroxynitrite is being consumed, there will be a backward diffusion of ONOOH to the bulk solution and after deprotonation will further react with CO_2, with an overall effect of a decrease on BTBE oxidation yields. Globally, the data support that bicarbonate will facilitate nitration of water-exposed tyrosine residues while it will inhibit nitration of tyrosine residues buried in transmembrane domains or associated to lipoprotein environments.

An interesting observation of this work was that transition metal complexes were capable of significantly enhancing peroxynitrite-dependent BTBE nitration (Table 2 and Figure 6). In particular, hemin and Mn-tccp were strong catalyzers. Hemin is extremely hazardous when it is released from its natural anchor, the globin moiety, as observed in a variety of pathophysiological conditions and aged red blood cells (*58*). Being a hydrophobic molecule, hemin has a high affinity for cell membranes, intercalating into the phospholipid bilayer, and can participate in oxidation and nitration reactions (*17*, *59*). In turn, Mn-tccp (also known as Mn-tbap) and other Mn porphyrins have been extensively used as SOD mimics and peroxynitrite reductases. While peroxynitrite-mediated Mn-tccp-catalyzed nitration was reported for tyrosine, the presence of water-soluble reductants such as glutathione, ascorbate, and uric acid inhibits the process due to their fast reaction with the $O{=}Mn^{4+}$ species formed by peroxynitrite (see eq 3); however, these reductants will not penetrate to membranes, and therefore the prooxidant actions in hydrophobic environments of $O{=}Mn^{4+}$−tccp and also $O{=}Fe^{4+}$−hemin can be more pronounced (*35*) and may explain part of their toxicity. For both hemin and Mn-tccp, nitration yields are greatly enhanced (Figure 6), indicating that the metal complexes were in close proximity to BTBE and support a reaction chemistry under which the transition metal ($Me^{3+}X$; eq 3) serves as a Lewis acid facilitating the formation of a transient complex with peroxynitrite ($ONOO{-}Me^{3+}X$); in this complex the O−O bond is weakened and undergoes homolysis to $^\bullet NO_2$ plus a high oxidation state oxo−metal intermediate (*1*) that efficiently promotes the one-electron oxidation of BTBE to its corresponding phenoxyl radical ($BTBE^\bullet$):

$$ONOO^- + Me^{3+}X \rightarrow ONOO{-}Me^{3+}X \rightarrow {}^\bullet NO_2 + {}^\bullet O{-}Me^{3+}X \rightarrow {}^\bullet NO_2 + O{=}Me^{4+}X \quad (3)$$

$$BTBE(H) + O{=}Me^{4+}X \rightarrow BTBE^\bullet + Me^{3+}X + OH^- \quad (4)$$

$$BTBE^\bullet + {}^\bullet NO_2 \rightarrow 3\text{-}NO_2\text{-}BTBE \quad (5)$$

This mechanism (eqs 3−5) is further supported by the pH dependency of the nitration yields in the presence of transition metal complexes (Figure 8), which is completely different than in their absence (Figure 6) and totally consistent with the higher stability of oxo−metal complexes at alkaline pH (*60*), which increase their oxidation efficiency to BTBE and consistent with previous data (*17*, *59*).

Nitration and dimerization of the hydrophobic tyrosine analogue were observed both in the absence (Figure 3) and in the presence (Figure 6) of transition metal complexes in both saturated (DLPC and DMPC) and polyunsaturated fatty acid-containing liposomes (egg and soybean PC). Polyunsaturated fatty acids are good targets of strong oxidants such as $^\bullet OH$ and oxo−metal complexes. Moreover, in both egg and soybean PC liposomes (30 mM) the concentration of polyunsaturated fatty acids (7.3 and 17 mM, respectively) (*39*) is much higher than that of BTBE (0.3 mM) and would out compete for the reaction with peroxynitrite-derived radicals known to lead to lipid peroxidation (*36*) and nitration (*37*). Thus, considering simple competition kinetics a profound inhibition in BTBE oxidations in egg and soybean PC liposomes would be expected, unless BTBE oxidation is associated to the lipid oxidation process,; i.e., lipid-derived radicals promoting one-electron oxidation of BTBE to the corresponding BTBE (phenoxyl) radical ($E^{\circ\prime} = +0.88$ V) (*61*). This is possible with a highly oxidizing intermediate such as alkoxyl radical ($E^{\circ\prime} = +1.76$ V) (*62*) and maybe also with the less reactive peroxyl radical ($E^{\circ\prime} = +1.02$ V) (*63*). Once formed, the BTBE phenoxyl radical would react with $^\bullet NO_2$ ($k > 10^9\ M^{-1}\ s^{-1}$) or with another BTBE phenoxyl radical (this latter indicated by the significant increase on

dimerization yields in egg PC liposomes; Figure 3B). $^{\bullet}NO_2$ could also be consumed by lipid radicals to yield nitro lipids as the reaction is also close to diffusion-controlled; thus, the influence of BTBE (or tyrosine-containing peptides and proteins) on the extents of lipid nitration arises as a relevant issue for future studies.[6] The role of lipid peroxidation in BTBE oxidation is supported by a significant decrease on nitration and dimerization (~50%) by incubation of reaction mixtures under low oxygen tension (unpublished data).

BTBE is relatively easy to synthesize, is stable, and can be readily utilized as a probe to perform a wide range of studies on tyrosine nitration in hydrophobic environments. BTBE incorporated into liposomes represents a model system to study a variety of factors that may control nitration processes in biomembranes, including the role of aqueous and lipid-soluble free radical scavengers and catalyzers. In this regard, in addition to the method that involves separation of BTBE-derived products with the more demanding HPLC-based techniques (Figure 1A), the protocol presented herein using deoxycholate solubilization of saturated fatty acid-containing liposomes followed by direct spectrophotometric determination of 3-nitro-BTBE (Figure 1B) proved to be simple and reproducible (Figures 1C and 5). On the other hand, we have successfully incorporated BTBE to both red blood cell membranes and lipoproteins (unpublished data), which opens the possibility of its use as a tracer molecule to follow nitration processes in more complex biochemical/biological systems. As an option to BTBE, tyrosine-containing transmembrane peptides have also been synthesized and incorporated into liposomes (*55*). While the structure and reaction chemistry in these peptides can more closely reflect that of membrane proteins (*55*, *64*) in comparison to BTBE, their synthesis is a more complex endeavor; moreover, they are unlikely to be incorporated into biological membranes or lipoproteins. Thus, BTBE and tyrosine-containing transmembrane peptides constitute complementary probes. For example, studies of tyrosine hydroxylation in peptides containing residues at different depths in the membrane will assist in defining the relevance of ONOOH homolysis in the aqueous vs lipid phase, as $^{\bullet}OH$ diffusing from the bulk solution will mainly react with residues located near the liposome surface (*52*).

In summary, BTBE was a useful probe to define peroxynitrite-dependent mechanisms of biomembrane nitration and provided new information regarding factors, such as CO_2 and hemin, that will down- or upmodulate, respectively, nitration and other oxidation processes in hydrophobic environments. In addition, due to the minimal diffusion of $^{\bullet}OH$, the detection of 3-hydroxy-BTBE supports the "site-specific" homolysis of ONOOH to $^{\bullet}OH$ and $^{\bullet}NO_2$ in the immediacy or even inside the phospholipid bilayer and consistent with the previously reported larger yields of tyrosine-containing transmembrane peptide nitration for tyrosine residues located deeper in the bilayer (*55*). Further studies utilizing BTBE incorporated into liposomes, cell membranes, and lipoproteins will serve to further unravel factors that control peroxynitrite-dependent as well as independent (i.e., via hemin and metalloproteins) protein and lipid nitration.

[6] $^{\bullet}NO_2$ is a one-electron oxidant and could potentially oxidize BTBE (Supporting Information, Table 1S) or polyunsaturated fatty acids ($k = 10^5\ M^{-1}\ s^{-1}$); however, these rate constant values are relatively low, and in our system $^{\bullet}NO_2$ will preferentially react with BTBE- or lipid-derived radical species.

ACKNOWLEDGMENT

We thank Joy Joseph (Medical College of Wisconsin) for the synthesis of BTBE, 3-nitro-BTBE, and 3,3′-di-BTBE and Virginia Lopez (Universidad de la República) for helpful discussion on mass spectrometry analysis of 3-hydroxy-BTBE.

SUPPORTING INFORMATION AVAILABLE

ESR-spin trapping data and kinetic simulations that support a free radical mechanism of BTBE oxidation by peroxynitrite. This material is available free of charge via the Internet at http://pubs.acs.org.

REFERENCES

1. Radi, R. (2004) Nitric oxide, oxidants, and protein tyrosine nitration, *Proc. Natl. Acad. Sci. U.S.A. 101*, 4003−4008.
2. Estevez, A. G., Crow, J. P., Sampson, J. B., Reiter, C., Zhuang, Y., Richardson, G. J., Tarpey, M. M., Barbeito, L., and Beckman, J. S. (1999) Induction of nitric oxide-dependent apoptosis in motor neurons by zinc-deficient superoxide dismutase, *Science 286*, 2498−2500.
3. Ischiropoulos, H. (2003) Oxidative modifications of alpha-synuclein, *Ann. N.Y. Acad. Sci. 991*, 93−100.
4. Radi, R., Peluffo, G., Alvarez, M. N., Naviliat, M., and Cayota, A. (2001) Unraveling peroxynitrite formation in biological systems, *Free Radical Biol. Med. 30*, 463−88.
5. Beckman, J. S., Beckman, T. W., Chen, J., Marshall, P. A., and Freeman, B. A. (1990) Apparent hydroxyl radical production by peroxynitrite: implications for endothelial injury from nitric oxide and superoxide, *Proc. Natl. Acad. Sci. U.S.A. 87*, 1620−1624.
6. Radi, R., Beckman, J. S., Bush, K. M., and Freeman, B. A. (1991) Peroxynitrite oxidation of sulfhydryls. The cytotoxic potential of superoxide and nitric oxide, *J. Biol. Chem. 266*, 4244−4250.
7. Augusto, O., Gatti, R. M., and Radi, R. (1994) Spin-trapping studies of peroxynitrite decomposition and of 3-morpholinosydnonimine *N*-ethylcarbamide autooxidation: direct evidence for metal-independent formation of free radical intermediates, *Arch. Biochem. Biophys. 310*, 118−125.
8. Goldstein, S., Czapski, G., Lind, J., and Merenyi, G. (2000) Tyrosine nitration by simultaneous generation of (.)NO and O−(2) under physiological conditions. How the radicals do the job, *J. Biol. Chem. 275*, 3031−3036.
9. Lymar, S. V., and Hurst, J. K. (1995) Rapid reaction between peroxynitrite ion and carbon dioxide: implications for biological activity, *J. Am. Chem. Soc 117*, 8867−8868.
10. Bonini, M. G., Radi, R., Ferrer-Sueta, G., Ferreira, A. M., and Augusto, O. (1999) Direct EPR detection of the carbonate radical anion produced from peroxynitrite and carbon dioxide, *J. Biol. Chem. 274*, 10802−10806.
11. Lymar, S. V., Jiang, Q., and Hurst, J. K. (1996) Mechanism of carbon dioxide-catalyzed oxidation of tyrosine by peroxynitrite, *Biochemistry 35*, 7855−7861.
12. Lymar, S. V., Schwarz, H. A., and Czapski, G. (2000) Medium effects on reactions of the carbonate radicals with thiocyanate, iodide and ferrocyanide ions., *Radiat. Phys. Chem. 59*, 387−392.
13. Romero, N., Denicola, A., Souza, J. M., and Radi, R. (1999) Diffusion of peroxynitrite in the presence of carbon dioxide, *Arch. Biochem. Biophys. 368*, 23−30.
14. Stanbury, D. M. (1989) Reduction potencials involving inorganic free radicals in aqueous solutions., *Adv. Inorg. Chem. 33*, 69−138.
15. van der Vliet, A., Eiserich, J. P., O'Neill, C. A., Halliwell, B., and Cross, C. E. (1995) Tyrosine modification by reactive nitrogen species: a closer look, *Arch. Biochem. Biophys. 319*, 341−349.

16. Herzog, J., Maekawa, Y., Cirrito, T. P., Illian, B. S., and Unanue, E. R. (2005) Activated antigen-presenting cells select and present chemically modified peptides recognized by unique CD4 T cells, *Proc. Natl. Acad. Sci. U.S.A. 102*, 7928−7933.
17. Bian, K., Gao, Z., Weisbrodt, N., and Murad, F. (2003) The nature of heme/iron-induced protein tyrosine nitration, *Proc. Natl. Acad. Sci. U.S.A. 100*, 5712−5717.
18. Batthyany, C., Souza, J. M., Duran, R., Cassina, A., Cervenansky, C., and Radi, R. (2005) Time course and site(s) of cytochrome *c* tyrosine nitration by peroxynitrite, *Biochemistry 44*, 8038−8046.
19. Zhang, R., Brennan, M. L., Shen, Z., MacPherson, J. C., Schmitt, D., Molenda, C. E., and Hazen, S. L. (2002) Myeloperoxidase functions as a major enzymatic catalyst for initiation of lipid peroxidation at sites of inflammation, *J. Biol. Chem. 277*, 46116−46122.
20. Ferrer-Sueta, G., Vitturi, D., Batinic-Haberle, I., Fridovich, I., Goldstein, S., Czapski, G., and Radi, R. (2003) Reactions of manganese porphyrins with peroxynitrite and carbonate radical anion, *J. Biol. Chem. 278*, 27432−27438.
21. Ischiropoulos, H., Zhu, L., Chen, J., Tsai, M., Martin, J. C., Smith, C. D., and Beckman, J. S. (1992) Peroxynitrite-mediated tyrosine nitration catalyzed by superoxide dismutase, *Arch. Biochem. Biophys. 298*, 431−437.
22. Santos, C. X., Bonini, M. G., and Augusto, O. (2000) Role of the carbonate radical anion in tyrosine nitration and hydroxylation by peroxynitrite, *Arch. Biochem. Biophys. 377*, 146−152.
23. Beckman, J. S., Ischiropoulos, H., Zhu, L., van der Woerd, M., Smith, C., Chen, J., Harrison, J., Martin, J. C., and Tsai, M. (1992) Kinetics of superoxide dismutase- and iron-catalyzed nitration of phenolics by peroxynitrite, *Arch. Biochem. Biophys. 298*, 438−445.
24. Daiber, A., Bachschmid, M., Beckman, J. S., Munzel, T., and Ullrich, V. (2004) The impact of metal catalysis on protein tyrosine nitration by peroxynitrite, *Biochem. Biophys. Res. Commun. 317*, 873−881.
25. Mallozzi, C., Di Stasi, A. M., and Minetti, M. (1997) Peroxynitrite modulates tyrosine-dependent signal transduction pathway of human erythrocyte band 3, *FASEB J. 11*, 1281−1290.
26. Velsor, L. W., Ballinger, C. A., Patel, J., and Postlethwait, E. M. (2003) Influence of epithelial lining fluid lipids on NO_2-induced membrane oxidation and nitration, *Free Radical Biol. Med. 34*, 720−733.
27. Murray, J., Taylor, S. W., Zhang, B., Ghosh, S. S., and Capaldi, R. A. (2003) Oxidative damage to mitochondrial complex I due to peroxynitrite: identification of reactive tyrosines by mass spectrometry, *J. Biol. Chem. 278*, 37223−37230.
28. Viner, R. I., Ferrington, D. A., Williams, T. D., Bigelow, D. J., and Schoneich, C. (1999) Protein modification during biological aging: selective tyrosine nitration of the SERCA2a isoform of the sarcoplasmic reticulum Ca^{2+}-ATPase in skeletal muscle, *Biochem. J. 340*, 657−669.
29. Ji, Y., Neverova, I., Van Eyk, J. E., and Bennet, B. M. (2006) Nitration of tyrosine 92 mediates the activation of rat microsomal glutathione-S-transferase by peroxynitrite, *J. Biol. Chem. 281*, 1986−1991.
30. Shao, B., Bergt, C., Fu, X., Green, P., Voss, J. C., Oda, M. N., Oram, J. F., and Heinecke, J. W. (2005) Tyrosine 192 in apolipoprotein A-I is the major site of nitration and chlorination by myeloperoxidase, but only chlorination markedly impairs ABCA1-dependent cholesterol transport, *J. Biol. Chem. 280*, 5983−5993.
31. Zhang, H., Joseph, J., Feix, J., Hogg, N., and Kalyanaraman, B. (2001) Nitration and oxidation of a hydrophobic tyrosine probe by peroxynitrite in membranes: comparison with nitration and oxidation of tyrosine by peroxynitrite in aqueous solution, *Biochemistry 40*, 7675−7686.
32. Denicola, A., Souza, J. M., and Radi, R. (1998) Diffusion of peroxynitrite across erythrocyte membranes, *Proc. Natl. Acad. Sci. U.S.A. 95*, 3566−3571.
33. Marla, S. S., Lee, J., and Groves, J. T. (1997) Peroxynitrite rapidly permeates phospholipid membranes, *Proc. Natl. Acad. Sci. U.S.A. 94*, 14243−14248.
34. Goss, S. P., Singh, R. J., Hogg, N., and Kalyanaraman, B. (1999) Reactions of *NO, $*NO_2$ and peroxynitrite in membranes: physiological implications, *Free Radical Res. 31*, 597−606.
35. Trostchansky, A., Ferrer-Sueta, G., Batthyany, C., Botti, H., Batinic-Haberle, I., Radi, R., and Rubbo, H. (2003) Peroxynitrite flux-mediated LDL oxidation is inhibited by manganese porphyrins in the presence of uric acid, *Free Radical Biol. Med. 35*, 1293−300.
36. Radi, R., Beckman, J. S., Bush, K. M., and Freeman, B. A. (1991) Peroxynitrite-induced membrane lipid peroxidation: the cytotoxic potential of superoxide and nitric oxide, *Arch. Biochem. Biophys. 288*, 481−487.
37. Rubbo, H., Radi, R., Trujillo, M., Telleri, R., Kalyanaraman, B., Barnes, S., Kirk, M., and Freeman, B. A. (1994) Nitric oxide regulation of superoxide and peroxynitrite-dependent lipid peroxidation. Formation of novel nitrogen-containing oxidized lipid derivatives, *J. Biol. Chem. 269*, 26066−26075.
38. Buege, J. A., and Aust, S. D. (1978) Microsomal lipid peroxidation, *Methods Enzymol. 52*, 302−310.
39. New, R. R. C. (1989) *Liposomes: a Practical Approach*, IRL Press at Oxford University Press, New York.
40. Huang, C., and Mason, J. T. (1978) Geometric packing constraints in egg phosphatidylcholine vesicles, *Proc. Natl. Acad. Sci. U.S.A. 75*, 308−310.
41. Khairutdinov, R. F., Coddington, J. W., and Hurst, J. K. (2000) Permeation of phospholipid membranes by peroxynitrite, *Biochemistry 39*, 14238−14249.
42. Lide, D. R. (1990) *Handbook of Chemistry and Physics*, 71st ed., CRC Press, Boca Raton, FL.
43. Mendes, P. (1997) Biochemistry by numbers: simulation of biochemical pathways with Gepasi 3, *Trends Biochem. Sci. 22*, 361−363.
44. Schopfer, F. J., Baker, P. R., Giles, G., Chumley, P., Batthyany, C., Crawford, J., Patel, R. P., Hogg, N., Branchaud, B. P., Lancaster, J. R., Jr., and Freeman, B. A. (2005) Fatty acid transduction of nitric oxide signaling. Nitrolinoleic acid is a hydrophobically stabilized nitric oxide donor, *J. Biol. Chem. 280*, 19289−19297.
45. Lauridsen, C., Leonard, S. W., Griffin, D. A., Liebler, D. C., McClure, T. D., and Traber, M. G. (2001) Quantitative analysis by liquid chromatography-tandem mass spectrometry of deuterium-labeled and unlabeled vitamin E in biological samples, *Anal. Biochem. 289*, 89−95.
46. Mottier, P., Gremaud, E., Guy, P. A., and Turesky, R. (2002) Comparison of gas chromatography-mass spectrometry and liquid chromatography-tandem mass spectrometry methods to quantify alpha-tocopherol and alpha-tocopherolquinone levels in human plasma, *Anal. Biochem. 301*, 128−135.
47. Solar, S., Solar, W., and Getoff, N. (1984) Reactivity of OH with tyrosine in aqueous solution studie by pulse radiolysis, *J. Phys. Chem. 88*, 2091−2095.
48. Trujillo, M., Folkes, L., Bartesaghi, S., Kalyanaraman, B., Wardman, P., and Radi, R. (2005) Peroxynitrite-derived carbonate and nitrogen dioxide radicals readily react with lipoic and dihydrolipoic acid, *Free Radical Biol. Med. 39*, 279−288.
49. Bartesaghi, S., Trujillo, M., Denicola, A., Folkes, L., Wardman, P., and Radi, R. (2004) Reactions of desferrioxamine with peroxynitrite-derived carbonate and nitrogen dioxide radicals, *Free Radical Biol. Med. 36*, 471−483.
50. Denicola, A., Freeman, B. A., Trujillo, M., and Radi, R. (1996) Peroxynitrite reaction with carbon dioxide/bicarbonate: kinetics and influence on peroxynitrite-mediated oxidations, *Arch. Biochem. Biophys. 333*, 49−58.
51. Alvarez, B., Ferrer-Sueta, G., Freeman, B. A., and Radi, R. (1999) Kinetics of peroxynitrite reaction with amino acids and human serum albumin, *J. Biol. Chem. 274*, 842−848.
52. Barber, D. J. W., and Thomas, J. K (1978) Reactions of radicals with lecithin bilayers, *Radiat. Res. 74*, 51−65.
53. Vanderkooi, J. M., and Callis, J. B. (1974) Pyrene. A probe of lateral diffusion in the hydrophobic region of membranes, *Biochemistry 13*, 4000−4006.
54. Sackmann, E., Trauble, H., Galla, H., and Overath, P. (1973) Lateral diffusion, protein mobility and phase transitions in *Escherichia coli* membranes. A spin label study, *Biochemistry 12*, 5360−5369.
55. Zhang, H., Bhargava, K., Keszler, A., Feix, J., Hogg, N., Joseph, J., and Kalyanaraman, B. (2003) Transmembrane nitration of hydrophobic tyrosyl peptides. Localization, characterization, mechanism of nitration, and biological implications, *J. Biol. Chem. 278*, 8969−8978.
56. Moller, M., Botti, H., Batthyany, C., Rubbo, H., Radi, R., and Denicola, A. (2005) Direct measurement of nitric oxide and oxygen partitioning into liposomes and low-density lipoprotein, *J. Biol. Chem. 280*, 8850−8854.

57. Czapski, G. (1999) Acidity of the carbonate radical, *J. Phys. Chem. A 103*, 3447−3450.
58. Sullivan, S. G., Baysal, E., and Stern, A. (1992) Inhibition of hemin-induced hemolysis by desferrioxamine: binding of hemin to red cell membranes and the effects of alteration of membrane sulfhydryl groups, *Biochim. Biophys. Acta 1104*, 38−44.
59. Thomas, D. D., Espey, M. G., Vitek, M. P., Miranda, K. M., and Wink, D. A. (2002) Protein nitration is mediated by heme and free metals through Fenton-type chemistry: an alternative to the NO/O_2^- reaction, *Proc. Natl. Acad. Sci. U.S.A. 99*, 12691−12696.
60. Ferrer-Sueta, G., Batinic-Haberle, I., Spasojevic, I., Fridovich, I., and Radi, R. (1999) Catalytic scavenging of peroxynitrite by isomeric Mn(III) *N*-methylpyridylporphyrins in the presence of reductants, *Chem. Res. Toxicol. 12*, 442−449.
61. Stubbe, J., and van der Donk, W. A. (1998) Protein radicals in enzyme catalysis, *Chem. Rev. 98*, 705−762.
62. Merenyi, G., Lind, J., and Goldstein, S. (2002) Thermochemical properties of alpha-hydroxy-alkoxyl radicals in aqueous solution, *J. Phys. Chem. A 106*, 11127−11129.
63. Jonsson, M. (1996) Thermochemical properties of peroxides and peroxyl radicals, *J. Phys. Chem. 100*, 6814−6818.
64. Zhang, H., Xu, Y., Joseph, J., and Kalyanaraman, B. (2005) Intramolecular electron transfer between tyrosyl radical and cysteine residue inhibits tyrosine nitration and induces thiyl radical formation in model peptides with MPO, H_2O_2 and NO_2^-: EPR spin trapping studies, *J. Biol. Chem. 280*, 40684−40698.

BI060363X